

THE SOUTH GEORGIA WAVE EXPERIMENT

A Means for Improved Analysis of Gravity Waves and Low-Level Wind Impacts Generated from Mountainous Islands

D. R. JACKSON, A. GADIAN, N. P. HINDLEY, L. HOFFMANN, J. HUGHES, J. KING, T. MOFFAT-GRIFFIN,
A. C. MOSS, A. N. ROSS, S. B. VOSPER, C. J. WRIGHT, AND N. J. MITCHELL

New observations at South Georgia (an extremely intense source of gravity waves) are used to evaluate model simulations of gravity waves and wakes.

Gravity waves (GWs), or buoyancy waves, play an important role in the atmosphere. The waves can modulate small-scale tropospheric weather phenomena, such as convection, and when they break they contribute to mixing of constituents. The waves can propagate to great heights, depositing both energy and momentum into the stratosphere and mesosphere when they break there. This momentum deposition results in a “drag” on the wind that is significant in the stratosphere and so large in the mesosphere that it closes the zonal jets and forces a global pole-to-pole meridional circulation that cools the summer mesopause to be the coldest place on Earth (e.g., Lübken and von Zahn 1991). GWs are thus fundamental to the structure and dynamics of the atmosphere.

Recent satellite observations have suggested that strong winds blowing over small mountainous islands can be a regular source of intense orographic GWs (mountain waves) (e.g., Hoffmann et al. 2016). The momentum carried by these GWs from mountainous islands is believed to have a climatologically significant impact on the circulation of the atmosphere. For

example, the importance of the stratospheric wave drag at 60°S was recently highlighted by McLandress et al. (2012), who suggested that cold biases in the Southern Hemisphere stratospheric polar vortex, common to many climate models, might be associated with poor representation of the wave drag. South Georgia (54.5°S, 37°W) in the remote southern Atlantic Ocean is believed to be among the most intense source of such island GWs anywhere on Earth (e.g., Alexander et al. 2009).

As alluded to by McLandress et al. (2012), most global climate and numerical weather prediction (NWP) models, including the Met Office Unified Model (UM), suffer from what we can call the “small-island problem.” This arises because the source of the orographic GW drag is typically not explicitly resolved and instead is represented by parameterization (e.g., Palmer et al. 1986; McFarlane 1987; Alexander et al. 2010). Furthermore, it has become clear in recent years that the near-surface drag associated with mountain barriers and flow blocking dynamics is equally, if not more, important than the orographic

GW drag, and that parameterization schemes are also required to represent this missing drag in models (e.g., Lott and Miller 1997; Scinocca and McFarlane 2000; Webster et al. 2003). Processes associated with strongly stratified conditions such as upwind flow blocking, flow splitting, wake formation, and low-level wake breaking impart a drag on the flow at low levels (over depths similar to the mountain height; Wells et al. 2008a,b). As with mountain waves, these processes occur on horizontal length scales as small as the small islands (i.e., a few kilometers).

Our understanding of GWs is also poorly constrained by observations. Significant uncertainties remain about the nature and variability of the waves produced under different meteorological conditions. GWs tend to occur in isolated, intermittent wave packets whose amplitudes and fluxes of energy and momentum can be an order of magnitude greater than time-averaged values (e.g., Buhler 2003; Plougonven et al. 2013). This intermittency is important to quantify because large-amplitude GWs can behave very differently from ones of smaller amplitude (e.g., breaking at lower heights), and so use of averaged GW fluxes in parameterizations can be very misleading. Furthermore, a comprehensive study of GWs requires simultaneous observations of the same region using different methods. This is because in situ observations (e.g., from radiosondes or radar) offer very high vertical resolution observations of GWs, but only over a limited area. Satellite observations, on the other hand, do have the advantage of near-global coverage, but the vertical (horizontal) resolution of nadir (limb) sounding data is insufficient.

South Georgia is at the edge of the “hot spot” region of very large stratospheric GW momentum fluxes observed by satellites to extend over the southern Andes–Drake Passage–Antarctic Peninsula region in winter (e.g., Ern et al. 2011). It also lies in the associated “wake region” of increased stratospheric GW energies observed downwind (i.e., eastward) of the hot spot. These features make South Georgia the ideal natural laboratory around which to study mountainous-island GWs and their representation in models. Here we report results from the South Georgia Wave Experiment (SG-WEX), a major coordinated observational and modeling experiment to determine the nature and impacts of gravity waves generated by South Georgia. Goals of SG-WEX include a more comprehensive observational understanding of GWs (using radiosonde, radar, and satellite observations) and the associated development of gravity wave parameterizations to allow the effects from islands such as South Georgia to be better represented in the UM (e.g., Vosper 2015).

There is a long heritage of model- and observation-based GW studies. Fritts et al. (2016) and Fritts and Alexander (2003) provide good reviews. A major recent observation-based study is the Deep Propagating Gravity Wave Experiment (DEEPWAVE; Fritts et al. 2016), which used ground-based and aircraft observations covering the 0–100-km altitude range and focused on the New Zealand and Tasmanian GW hot spot regions. Studies based on DEEPWAVE have, for example, focused on GWs generated by the Auckland Islands (Eckermann et al. 2016) and the mesospheric response to such waves (Pautet et al. 2016). Another major recent study (Jiang et al. 2014) used reanalysis data to investigate contributions to the stratospheric wave drag from three neighboring orographic wave sources (Patagonian peaks in the Andes, the Antarctic Peninsula, and South Georgia). There is also a long tradition of studying the wake structure behind islands both experimentally (Smith and Grubišić 1993; Young and Zawislak 2006; Grubišić et al. 2015) and theoretically (Schär and Smith 1993; Grubišić et al. 1995; Schär and Durran 1997). SG-WEX is innovative because it confronts high-resolution model simulations with both radiosonde and satellite observations to identify the ability of the model to represent GWs, and also the associated low-level flow blocking, without parameterization. It also uses an innovative method to analyze GWs from 3D satellite temperature retrievals, as detailed in the “Gravity wave analysis” section. SG-WEX focuses on South Georgia and provides the first reported radiosonde observations from this location.

AFFILIATIONS: JACKSON—Met Office, Exeter, and University of Bath, Bath, United Kingdom; GADIAN, HUGHES, AND ROSS—University of Leeds, Leeds, United Kingdom; HINDLEY—University of Bath, Bath, and University of Leeds, Leeds, United Kingdom; HOFFMANN—Forschungszentrum Jülich, Jülich, Germany; KING AND MOFFAT-GRIFFIN—British Antarctic Survey, Cambridge, United Kingdom; MOSS, WRIGHT, AND MITCHELL—University of Bath, Bath, United Kingdom; VOSPER—Met Office, Exeter, and University of Leeds, Leeds, United Kingdom

CORRESPONDING AUTHOR: David Jackson, david.jackson@metoffice.gov.uk

The abstract for this article can be found in this issue, following the table of contents.

DOI:10.1175/BAMS-D-16-0151.1

In final form 9 November 2017

©2018 American Meteorological Society

For information regarding reuse of this content and general copyright information, consult the [AMS Copyright Policy](#).



This article is licensed under a [Creative Commons Attribution 4.0 license](#).

The remoteness and nature of South Georgia present several challenges for field observations. Access to the island is far from straightforward. During SG-WEX scientists and equipment were successfully transported to King Edward Point (KEP; see Fig. 1), the base for the radiosonde launches, by the fisheries protection vessel *Pharos*, which makes semiregular trips from the Falkland Islands.

Two radiosonde campaigns were held during 2015, one in summer and one in winter. The first ran from 7 to 23 January 2015, and the second ran from 13 June to 7 July 2015. There were twice-daily launches at 1100 and 2300 UTC as standard from KEP. There were also periods of intensive launches (up to one balloon every 4 h) to coincide with overpasses by the A-Train satellite constellation (L'Ecuyer and Jiang 2010) or when strong winds perpendicular to the spine of the island were forecast by the Met Office (conditions favorable for strong mountain wave activity).

The stormy weather of the island made for challenging conditions for launching balloons on several occasions, and the steep terrain surrounding KEP meant that for certain balloon trajectories it was not possible to maintain line-of-sight communication with the radiosondes, so some data were inevitably lost. Nevertheless, despite these challenges there were 89 successful radiosonde launches in total, with 46 of these reaching altitudes above 25 km. The data gathered as part of SG-WEX form a unique dataset: the first summer and winter radiosonde observations of the GW activity in a region poorly observed by in situ and ground-based instruments.

In this paper we present a case study from 5 July 2015. Satellite and analysis data indicate this date as one when GWs with very high momentum flux were observed, with South Georgia being the likely orographic source. We focus on dedicated radiosonde observations made on South Georgia, and satellite observations from the Advanced Infrared Sounder (AIRS) and the Advanced Scatterometer (ASCAT),

complemented and guided by high-resolution UM simulations of GW generation and propagation around the island. In the following sections we describe the UM and the various observations used, show the results, and summarize the results and their possible global implications.

MODEL AND OBSERVATIONAL DATA.

Unified Model. UM simulations were conducted using the latest version of the Even Newer Dynamics for General Atmospheric Modeling of the Environment dynamical core (ENDGame; Wood et al. 2014). The improved stability of ENDGame results in a more accurate treatment of resolved GW motion, as discussed by Shutts and Vosper (2011).

Global UM simulations were conducted at N512 resolution (corresponding to an approximate grid length of 25 km at midlatitudes) with 70 height-based vertical levels up to a height of 80 km above mean sea level (MSL). The simulations were initialized with Met Office operational analyses and integrated forward in time for 24 h. These forecasts were reinitialized every 24 h and used to supply lateral boundary conditions for high-resolution limited area configurations over South Georgia. The limited area domains were centered on South Georgia and extended approximately 1,200 km in the east–west direction and 900 km in the north–south direction. The grids were

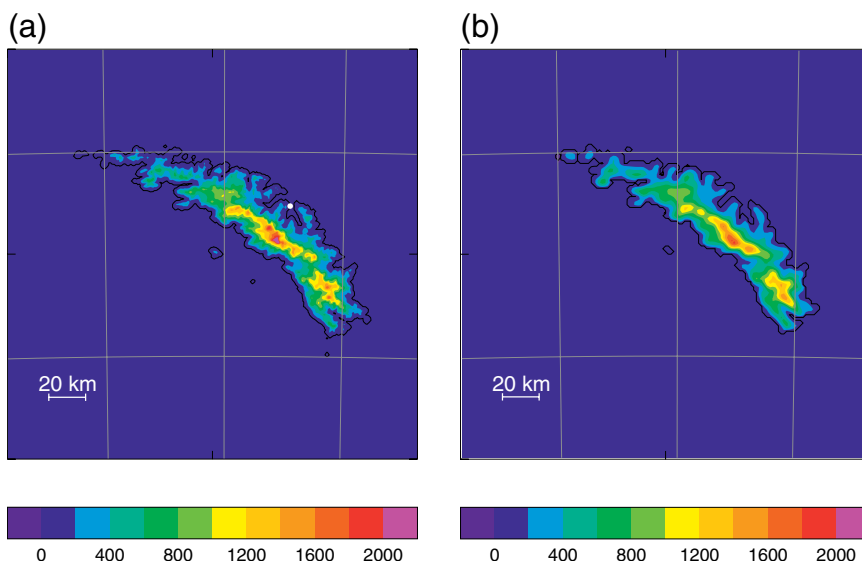


FIG. 1. The model orography for the UM limited-area simulations with (a) 750-m and (b) 1.5-km horizontal grid spacing. These data were created from SRTM digital terrain data with 3-arc-s resolution. Both panels show a zoomed-in view across South Georgia; the full extents of the model domains are considerably larger. Terrain heights are shown in meters (color contour interval: 400 m). Lines of constant latitude and longitude are shown with a 1° interval. The white dot in (a) marks the location of King Edward Point on the east coast.

defined relative to a rotated pole (at 35.5°N, 37.1°W) so as to make them close to Cartesian. Two such grids were used, with horizontal grid lengths of 750 m and 1.5 km. The model orography was created from the 3-arc-s resolution (~90 m) Shuttle Radar Topography Mission (SRTM) digital terrain dataset, averaged onto the model grid. On both grids the resulting orography contains much of the detail of the individual mountain peaks (see Fig. 1). These resolutions are designed to capture the local orographic generation of GWs and to simulate the low-level processes such as flow splitting, downslope winds, and wake generation. The simulations used 118 levels in the vertical within a deep model domain that extended into the mesosphere. The model lid was at 78 km MSL, with a damping layer applied above 58.5 km. The vertical grid spacing was less than 500 m from the surface to 20 km MSL, rising to 1 km at ~35 km, 2 km at ~60 km, and approximately 3 km at the model top. This grid has previously been shown to be sufficient to represent vertical propagation of GWs generated by South Georgia through the stratosphere (Vosper 2015). Given the high resolution, no additional GW parameterization was included in the limited-area simulations.

The 1.5-km simulations were conducted for the whole of both the summer and winter SG-WEX radiosonde campaigns (see the first section) and were free running, initialized once at the start of each run and then forced only by the lateral boundary conditions. Computing constraints meant that the 750-m simulations were used for selected shorter case studies only.

Observations. AIRS. AIRS, which flies on NASA's *Aqua* satellite, is a nadir sounder that measures the thermal emissions of atmospheric constituents. The data have been collected nearly continuously since September 2002. There are around 45 AIRS overpasses per week that cover a $5^\circ \times 5^\circ$ box over South Georgia. Radiance measurements in the 4- and 15- μm CO_2 bands are most suitable for observing gravity waves. Here, we use temperatures that have been retrieved using the methods described by Hoffmann and Alexander (2009). These retrievals focus on stratospheric temperature and have a horizontal resolution of around $13.5 \text{ km} \times 13.5 \text{ km}$ at nadir and $41 \text{ km} \times 21.4 \text{ km}$ at track edge, and a vertical resolution of 7–15 km. The dataset is sensitive to gravity waves with vertical wavelengths larger than about 15 km and horizontal wavelengths shorter than about 1,300 km. See Wright et al. (2017) for further discussion. The method to analyze the observed GW structure is detailed in the "Gravity wave analysis" section.

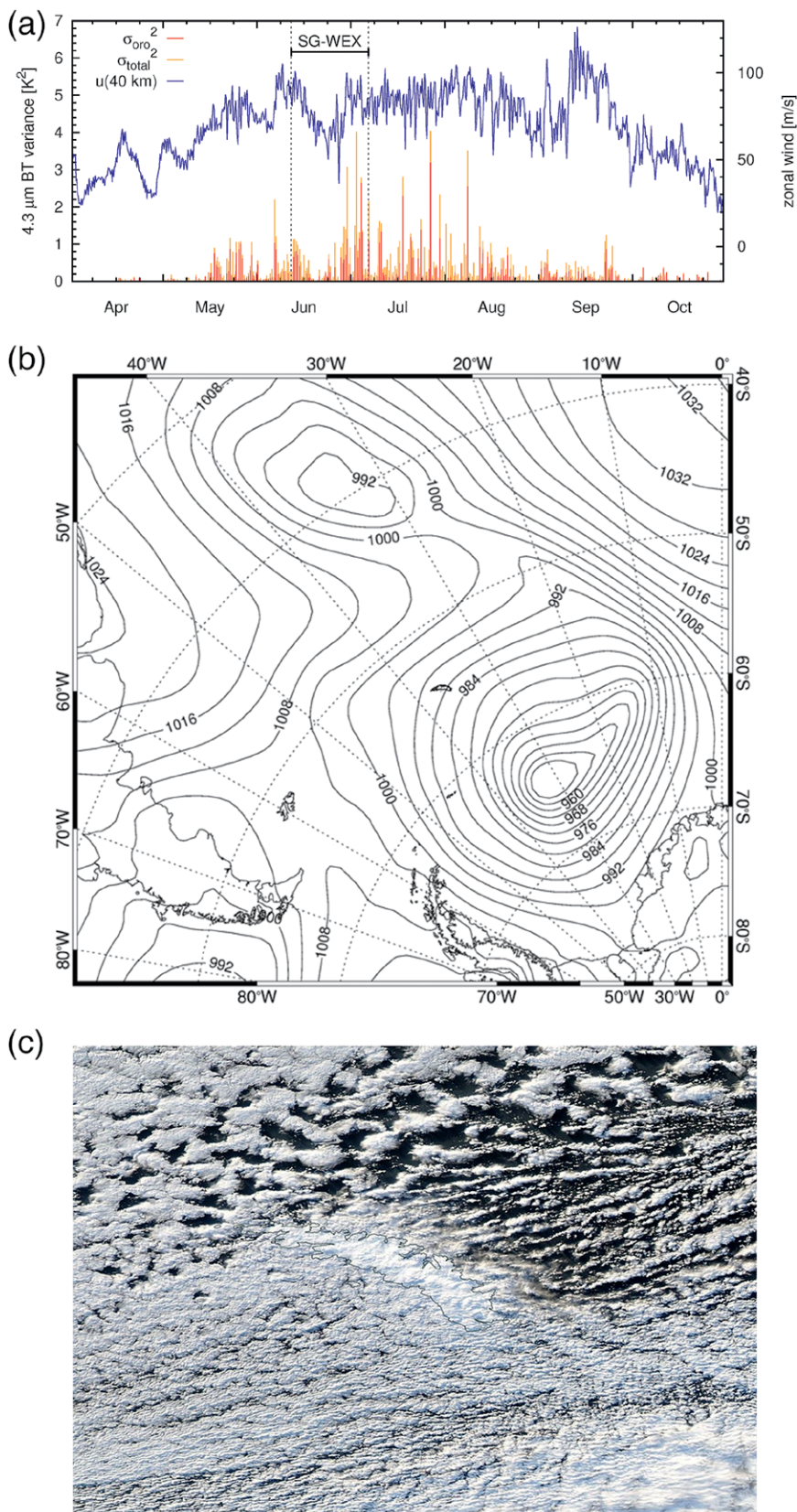
RADIOSONDES. Four launches of Vaisala RS92-SGP radiosondes were made on 5 July 2015, but only one reached stratospheric altitudes (at 0853 UTC). The radiosonde was launched with an 800-g helium-filled balloon in surface conditions where winds were in excess of 7.7 m s^{-1} . Strong winds during the wintertime cause the balloons to travel large horizontal distances (up to 650 km downwind during this campaign) before it bursts. Typically, we would expect a balloon of this type to reach burst altitudes in excess of 28 km. For this launch, however, the balloon burst just above 18 km. Data presented in the analysis are between 12 km (above the tropopause) and 18 km. The radiosonde data are composed of altitude profiles of temperature, wind speed, wind direction, pressure, humidity, and dewpoint at both 10- and 2-s resolution. The 2-s resolution data also contain the balloon ascent rate.

ASCAT. Winds derived from the ASCAT instruments allow us to evaluate the wake structure in the model. ASCAT instruments fly on board the *MetOp-A* and *MetOp-B* satellites, and the ASCAT data products (version 1.2) provide wind speed and direction at 10 m MSL along the satellite swath. The horizontal resolution is 25 km, and typically there are up to around eight passes a day over or close to South Georgia.

CASE STUDY, 5 JULY 2015. Figure 2a shows that AIRS observed three rather strong GW events during SG-WEX. The first two events were not attributed to South Georgia being the orographic source, but for 5 July 2015 this is the case. During the entire 2015 winter season, AIRS observed only four island wave events with similar levels of activity. Accordingly, 5 July 2015 is a very good day for a case study. Furthermore, because real-time forecasts suggested conditions favorable for strong mountain wave generation and deep upward propagation, an enhanced number of launches were performed.

On this day, the European Centre for Medium-Range Weather Forecasts (ECMWF) interim reanalysis (ERA-Interim) shows a deep (central pressure ~950 hPa) surface low pressure system to the south of South Georgia and a weak ridge of high pressure extending southward toward the island from the subtropical South Atlantic (see Fig. 2b). The pressure gradient associated with these features drove strong ($\sim 20 \text{ m s}^{-1}$) low-level westerly (i.e., cross barrier) winds in the vicinity of South Georgia that were conducive to strong mountain wave generation. Furthermore, wind speeds increased monotonically with height to around 80 m s^{-1} at 40 km (see Fig. 2a), while wind directions remained

within the southwesterly quadrant over this height range, providing favorable conditions for deep propagation of orographically generated waves into the stratosphere. Moderate Resolution Imaging Spectroradiometer (MODIS) imagery shows cloudiness upstream of the island and fewer clouds downstream, which may be evidence for subsidence in the wake region (Fig. 2c). Very clear wave activity is seen in AIRS data in two time slots (0314 and 1644 UTC) on either side of the 0853 UTC radiosonde launch. The satellite data show a large-scale wave over South Georgia during this day, and the radiosonde track passes directly through it. Unfortunately, in this case the relatively low maximum altitude achieved by the balloon means that the radiosonde cannot detect the



► **FIG. 2.** (a) Total GW activity in terms of 4.3- μm brightness temperature variances as observed by AIRS at 30–40-km altitude over South Georgia in Apr–Oct 2015 (orange) and the fraction of variance that is attributed to orographic wave activity from South Georgia (red). ERA-Interim 6-hourly zonal winds at about 40-km altitude are also shown. The methods and details of this analysis are described by Hoffmann et al. (2016). (b) ERA-Interim mean sea level pressure (hPa) at 0000 UTC 5 Jul 2015 over the South Atlantic. South Georgia is near the center of the figure. (c) MODIS true-color-corrected reflectance image around South Georgia (outlined) at 1645 UTC 5 Jul 2015 measured by the Aqua satellite.

longer-vertical-wavelength GWs that would lend themselves to direct comparison with the satellite data.

In the following we begin by describing the GWs seen by AIRS and compare these with the UM-simulated waves. The vertical GW structure is then further examined using measurements from the 0853 UTC radiosonde. These are again compared with the UM GWs.

Gravity wave analysis. The GW analysis of the AIRS retrievals detailed in the “Model and observational data” section is carried out using a three-dimensional (3D) Stockwell spectral transform (hereafter S-transform), as described by Wright et al. (2016, 2017). This builds on the 1D and 2D S-transforms previously used for GW analysis (Alexander and Barnet 2007; Hindley et al. 2016) and has the advantage that it addresses the strong cross-track bias problem inherent in the 1D and 2D approaches. The S-transform is used to measure GW amplitudes (in temperature), horizontal wavelengths, and directions of propagation from the AIRS data. To allow meaningful comparisons with the analysis of the satellite data, we apply the same techniques to the UM data.

Following the analysis of the AIRS data using the S-transform we still need to estimate the GW momentum flux. The 3D S-transform method allows us to directly measure the zonal, meridional, and vertical wavenumbers, so, unlike the commonly used method of Alexander et al. (2009), there is no need to assume zero phase speed or to use supplementary wind data. However, the method still assumes a long vertical extent and wavelength ($> \sim 20$ km) and a significant background wind speed ($> \sim 40$ m s⁻¹). The increasing wind speeds at stratospheric altitudes foster the propagation of gravity waves with long vertical wavelengths (e.g., Fritts and Alexander 2003), which are best visible to AIRS.

Gravity wave temperature perturbations T' are found by removing the background temperature state \bar{T} via a fourth-order polynomial fit method as described in Wright et al. (2017). The 3D S-transform then allows us to measure wave amplitude T' and zonal, meridional, and vertical wavenumbers k , l , and m (Wright et al. 2017). Then, using the relation from Ern et al. (2004), the momentum flux in the zonal and meridional directions (M_x, M_y) can be computed as

$$\begin{pmatrix} M_x \\ M_y \end{pmatrix} = \frac{\rho}{2} \left(\frac{g}{N} \right)^2 \left(\frac{T'}{\bar{T}} \right)^2 \frac{(k, l)}{m}, \quad (1)$$

where ρ is the background atmospheric density, g is acceleration due to gravity, and N is the Brunt-Väisälä frequency.

GRAVITY WAVES IN AIRS DATA AND THE UM. Figure 3 shows the momentum fluxes in the stratosphere (at 40 km MSL) computed from the GWs observed by AIRS and simulated by the UM at 1644 UTC 5 July 2015. The model results shown are for the 1.5-km simulation, but the equivalent results for the 750-m grid are very similar, which suggests that the 1.5-km simulation is sufficient. The momentum flux calculations are carried out at both the AIRS and UM resolutions, and we also analyze the UM data at AIRS resolution to indicate the impact of horizontal resolution. All analyses show enhanced momentum flux above the island, with much lower fluxes upstream and downstream, immediately to the east of the island. There is also enhanced momentum flux downstream to the northeast and southeast in a bow- or wake-shaped pattern, which suggests the presence of a quasi-stationary orographic GW field, generated by the strong westerly flow.

While the momentum flux patterns deduced from AIRS and the model are broadly similar, they do show a number of differences. The contrast between high-momentum flux over the island and low flux

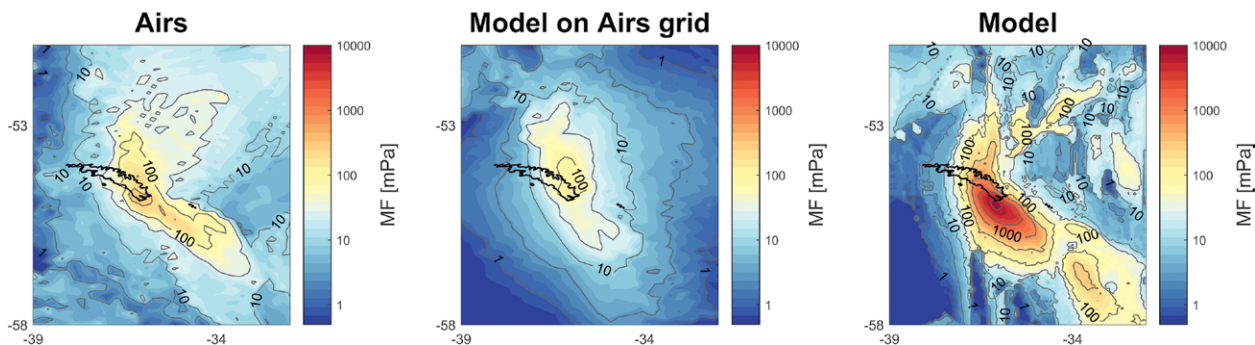


FIG. 3. GW momentum flux (mPa) at 40-km altitude at 1644 UTC 5 Jul 2015 calculated from (left) AIRS data, (center) UM data at AIRS resolution, and (right) UM data. The model results shown are from the 1.5-km simulation.

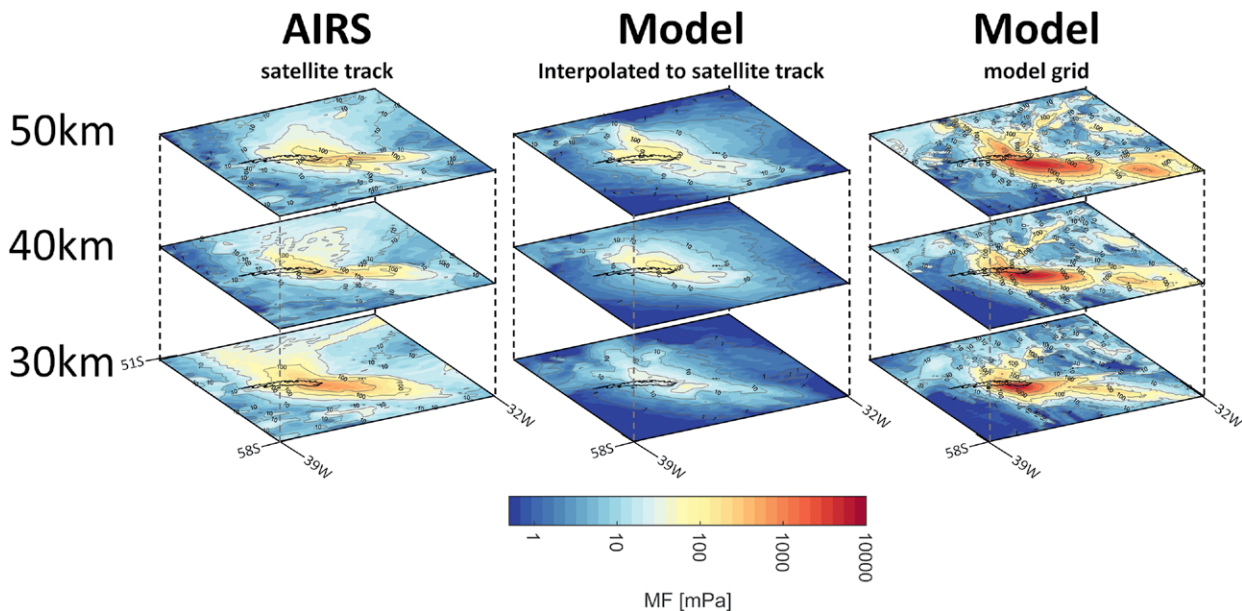


FIG. 4. GW momentum flux (mPa) at (bottom) 30, (middle) 40, and (top) 50 km MSL at 1644 UTC 5 Jul 2015 calculated from (left) AIRS data, (center) UM data at AIRS resolution, and (right) UM data.

downstream is very marked in the UM, whereas for AIRS the pattern is more smeared. As a result, the AIRS data show a maximum momentum flux of over 500 mPa centered over southeastern South Georgia, compared to considerably larger maximum values in the UM-based analysis (locally exceeding 10 Pa), while there is a distinct region of low flux (less than 3 mPa) downstream of the island in the UM analysis that is not seen in the AIRS analysis. High fluxes also extend downwind of the island, with maxima of over 100 mPa (for AIRS) and over 500 mPa (for UM) extending toward the southeast.

The different resolutions of the two datasets clearly influence the results. When the analysis of the model data is repeated at AIRS resolution, the spatial pattern becomes more comparable to that from the analysis made from the AIRS observations. Encouragingly, the momentum flux magnitudes in the “UM at AIRS resolution” analysis are similar to or a little smaller than those derived from the native-resolution AIRS data. Separate downscaling tests indicate similar-sized reductions in GW temperature amplitude and GW momentum flux with reduced resolution, so it appears that the change in momentum flux amplitudes seen when we use UM data at AIRS resolution is chiefly a result of peak amplitude reduction due to area averaging and a reduced ability to see very short horizontal wavelengths.

Based on the above discussion, it appears the UM is doing a good job of reproducing the AIRS observations and indeed may plausibly be representing the GW

pattern better because of the higher resolution: an example of this is the large zonal gradient in momentum flux seen going from the center to the east of the island.

Figure 4 compares GW momentum fluxes at different altitudes. The patterns are generally similar, which indicates that zero-phase-speed waves are dominant (as expected for an orographic source) and the lack of an obvious change of momentum flux with height indicates these waves are not breaking significantly within the 30–50-km region.

GRAVITY WAVES OBSERVED IN RADIOSONDE AND UM DATA.

In this section we examine the gravity waves as seen in three radiosonde-type datasets: the original 2-s-resolution data (vertical spacing of ~15 m), a so-called low-resolution radiosonde dataset averaged onto the UM vertical grid (approximately 400 m at 12 km MSL), and the UM simulated radiosonde profile, created by sampling the model data along the radiosonde trajectory. This examination provides insight as to whether errors in the model representation of the GWs can be explained in terms of vertical resolution.

Since the winds in the altitude region reach around $\sim 50 \text{ m s}^{-1}$, the analysis techniques used here will be valid (Zink and Vincent 2001). Initially, the perturbations of horizontal wind, vertical wind, and temperature between 12.6- and 18-km altitude were extracted by subtracting a second-order polynomial fitted to the original profile. This is standard practice for radiosonde gravity wave analyses (Vincent

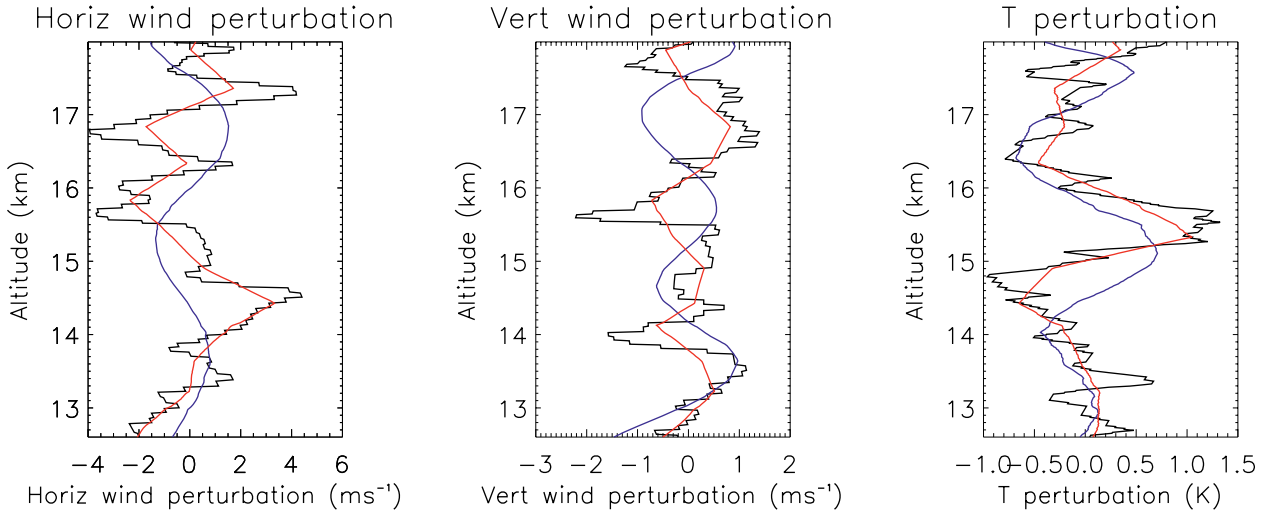


FIG. 5. (left) Horizontal wind perturbation, (center) vertical wind perturbation, and (right) temperature perturbation profiles for the 0853 UTC radiosonde (black line), the 1.5-km UM simulation (blue line), and the low-resolution radiosonde data (red line) on 5 Jul 2015.

et al. 1997) and work has shown that using other-order polynomials or filtering techniques like Kruse and Smith (2015) have little effect on the end result (Wang et al. 2005). The resulting perturbations are then assumed to be dominated by GW fluctuations. The radiosonde does not measure vertical velocity directly, but we assume that the ascent rate perturbation is equivalent to the vertical velocity perturbation w' (e.g., Geller and Gong 2010). The perturbation profiles are shown in Fig. 5.

There is reasonable agreement between the three profiles for the temperature perturbation, with the wave signal in the UM profile being slightly offset in altitude and of lower amplitude than in the radiosonde data. The horizontal wind perturbation profiles show a similar pattern to that observed in the temperature, with the UM perturbations again appearing offset in altitude and the agreement becoming poorer with increasing altitude. The model vertical perturbation profiles also appear to become increasingly out of phase with the radiosonde data at the higher end of the altitude range. This is consistent with the fact that small errors in the model wave field (e.g., in vertical wavelength) will result in a phase error that increased with altitude.

The radiosonde and model data were further analyzed to calculate the GW field kinetic (KE), potential (PE), and vertical energy (VE) density using Eqs. (2) from Lane et al. (2000). In these equations u' , v' , w' , and \check{T}' are the zonal, meridional, and vertical wind and the normalized temperature perturbations, respectively, and N is the Brunt–Väisälä frequency. The results are shown in Fig. 6:

$$\begin{aligned} \text{KE} &= \frac{1}{2} (u'^2 + v'^2), \\ \text{PE} &= \frac{1}{2} \frac{g^2}{N^2} \check{T}'^2, \\ \text{VE} &= \frac{1}{2} w'^2. \end{aligned} \quad (2)$$

Figure 6 shows that the low-resolution radiosonde data do not always capture the full magnitude of the energy densities. The factor of difference between the low-resolution and radiosonde data is similar to that of their respective horizontal resolutions (~85 km for the radiosonde data and ~135 km for the low-resolution data). The model data have a similar problem that is not as clearly linked to the vertical- and horizontal-resolution factors. The expected phase shift seen in the perturbation profiles is also seen here. This suggests that fine vertical and horizontal resolution is required, both for observations and for modeling, in order to obtain accurate estimates of the GW energy density.

The properties of the GW packets in the lower stratosphere have been examined in further detail by applying wavelet transforms (Morlet wavelet with $w_0 = 6$) to the temperature perturbation profiles. The results (Fig. 7) show that there is a dominant wave measured in all three profiles across the altitude range, which has a vertical wavelength of ~2.8 km. In the model this wave is centered around 1 km higher in altitude than that observed by the radiosonde, possibly consistent with the phase errors discussed earlier. The original radiosonde data capture wave activity down to shorter vertical wavelengths than

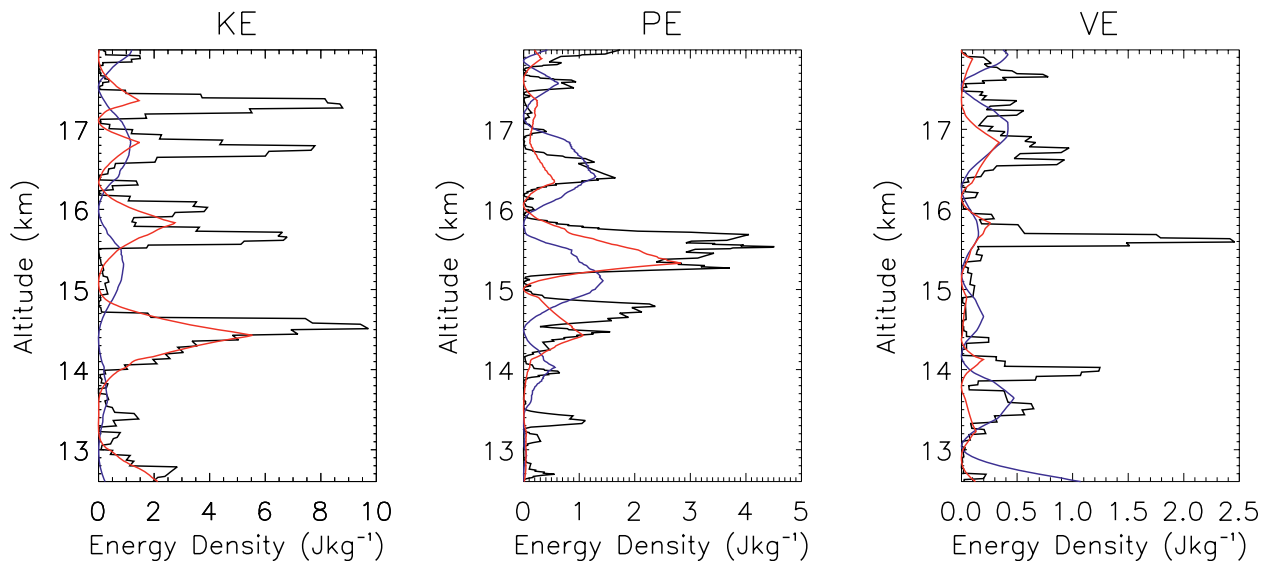


FIG. 6. (left) Kinetic energy density, (center) potential energy density, and (right) vertical energy density profiles for radiosonde (black line), UM (blue line), and low-resolution radiosonde (red line) on 5 Jul 2015. The y axis is altitude (km) and the x axis is energy density (J kg^{-1}).

the model-resolution data. From Fig. 6 it is clear that this is due to the higher variability, on shorter vertical scales, present in the full-resolution T' profile.

Impact on low-level winds. South Georgia also has significant impacts on the boundary layer flow during this case, with the generation of a low-level wake to the lee of the island. This is illustrated by Fig. 8a, which shows a composite of three ASCAT swaths (taken at 0921, 1015, and 1103 UTC 5 July). The scatterometer 10-m wind speeds upwind (to the west) of South Georgia are in the range of $16\text{--}20\text{ m s}^{-1}$ while a clear wake region of reduced speed ($\sim 10\text{ m s}^{-1}$) extends for several tens of kilometers to the lee, and there is

some apparent acceleration around the southern tip of the island. All these features resemble those presented by Hosking et al. (2015), and the latter (southern acceleration) also bears similarities to the tip jets observed around the southern end of Greenland (Doyle and Shapiro 1999; Moore and Renfrew 2005).

The equivalent model 10-m wind speeds are presented in Fig. 8b. Encouragingly, the simulated flow contains many of the features mentioned above in the ASCAT observations. The wake appears wider in the observations, but this is primarily due to the lower resolution of the ASCAT data.

The behavior of the wake around South Georgia has also been examined over the whole duration

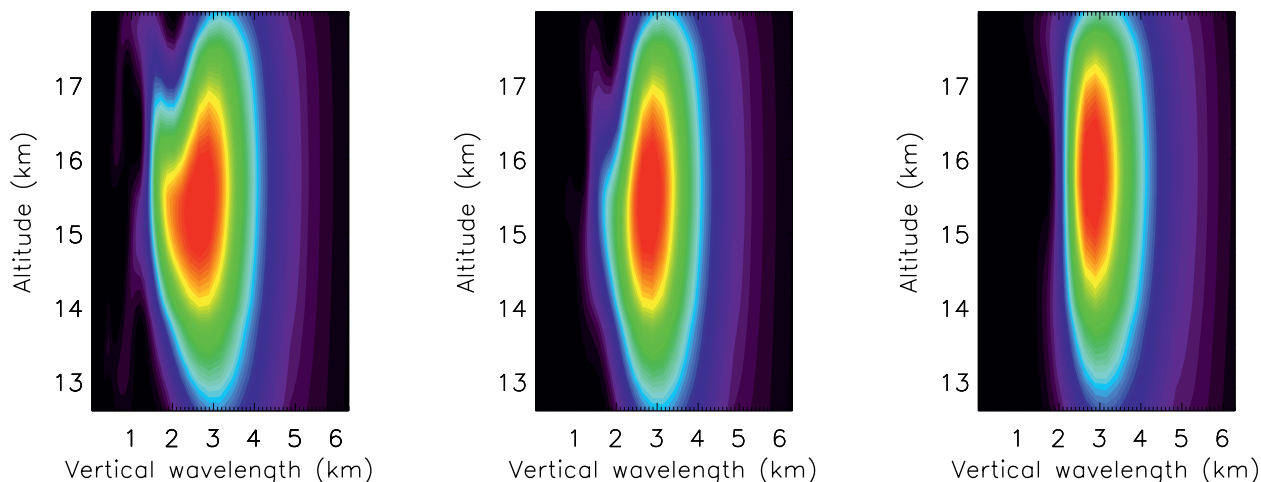


FIG. 7. Wavelet transforms of the temperature perturbation profiles for the (left) radiosonde, (center) low-resolution radiosonde, and (right) UM.

of the winter radiosonde campaign period during June and July 2015 by comparing the observed wakes in the ASCAT winds with those predicted

in the continuously running 1.5-km UM simulation. The wake effects have been extracted from the observations by removing estimates of the large-scale varying background

wind field derived from the global ERA-Interim (Dee et al. 2011). For the model, a background-flow field was obtained by running a companion set of simulations with the orography of South Georgia flattened to sea level, following Vosper (2015) and Vosper et al. (2016). The differences between the control and no-mountain wind field are then the perturbations due to the orography.

A simple measurement of the impact on the winds due to South Georgia is the fractional speed-up, defined as $\Delta s = (U - U_b)/U_b$, where U is the wind speed and U_b is the background wind speed. The spatial variation of the mean Δs , computed from the ASCAT data for periods where the (ERA-Interim) background wind direction over South Georgia was westerly (between 247.5° and 292.5°), is shown in Fig. 8c. The equivalent model wind field is shown in Fig. 8d. Both show a clear region of mean deceleration (a wake) to the east of South Georgia, with accompanying flanks where the flow is accelerated. Not surprisingly, the model contains more detail than can be detected by the satellite winds, but the similarity between the observations and model is nevertheless encouraging. Note that the regions of nonzero Δs far away and upstream of the island are associated with

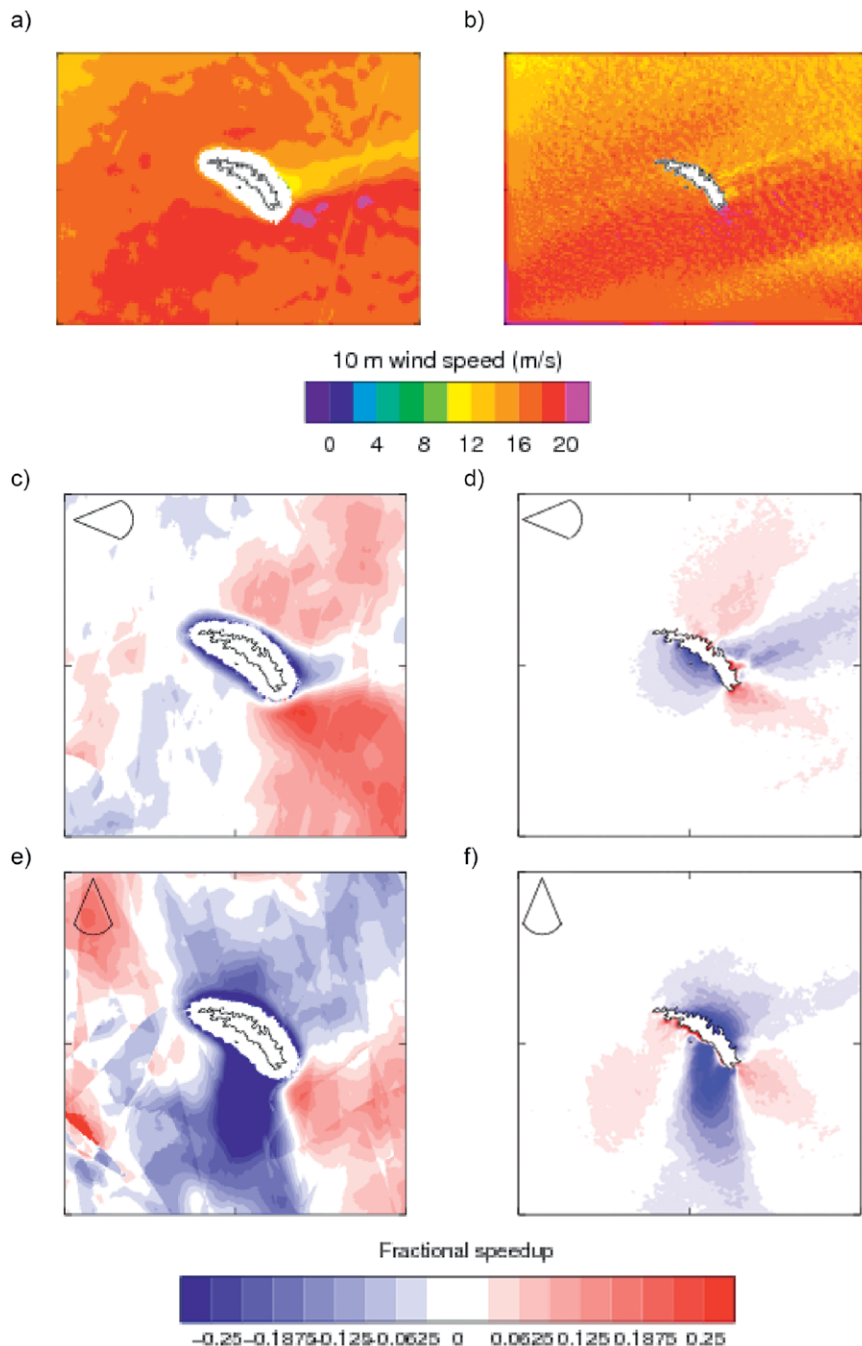


FIG. 8. The 10-m winds (a) measured by ASCAT near South Georgia on 5 Jul 2015 and (b) simulated by the UM on the 750-m grid. The ASCAT wind field in (a) is a composite of three scans taken at 0921, 1015, and 1103 UTC. The model wind field in (b) is an average over data at hourly intervals during the period 0900–1100 UTC from a simulation initialized at 0600 UTC. Also shown are the mean fractional speed-up Δs deduced from ASCAT winds for the Jun–Jul 2015 radiosonde campaign period during (c) westerly and (e) northerly flow and (d),(f) the respective equivalent 1.5-km model results. The segments in the upper-left corners of (c)–(f) indicate the range of wind directions considered.

differences between ASCAT winds and reanalysis and are unrelated to the wake effects. Figures 8e and 8f show the equivalent fractional speed-up for northerly flow (wind directions between 337.5° and 22.5°). The wake that extends to the south is very clear in both the observations and the model, and in this case an area of deceleration is also present on the upwind side of the island. This may be a sign of flow blocking, which happens upwind of mountain ranges when stable stratification is sufficiently strong. The level of agreement between the model and observations suggests that we can have some confidence in the use of high-resolution simulations such as these for understanding the impacts of these flows, such as wind-driven local ocean circulation (Hosking et al. 2015) and leeside temperature and moisture changes (Bannister and King 2015) and for developing parameterizations for use in coarse-resolution models (Vosper et al. 2016).

CONCLUSIONS. The preceding case study from 5 July 2015 illustrates the role of South Georgia in generating gravity waves and impacting the low-level flow.

An innovative method (the 3D S-transform) was used to analyze GWs from 3D AIRS temperature retrievals and high-resolution UM simulations. Both AIRS and the model simulations show evidence of orographic gravity waves being generated in a strong westerly flow, but also large resolution-dependent differences in the maximum GW momentum flux over and downstream of South Georgia. However, when account is taken of the differing resolutions of the AIRS data and the model, the GW patterns from both are much more alike. Vosper (2015) showed that the largest contribution to GW momentum flux over South Georgia is from horizontal wavelengths of around 30–60 km. Our results suggest that such wavelengths are present here and resolved by AIRS, but the GW momentum fluxes obtained from satellite measurements may be significantly underestimated when the wave fields contain important contributions from wavelengths that are too short to be detected. Accordingly, the model performs well in reproducing the AIRS observations and possibly provides a better estimate of the GW pattern and momentum fluxes because of its higher resolution.

Comparison between the dedicated radiosonde observations and the model also shows good agreement for temperature and horizontal wind perturbations in the lower stratosphere, although this degrades with increasing altitude. The model predictions become out of phase with the radiosonde measurements at the higher end of the altitude range. Wavelet transforms

show that there is one dominant vertical wavelength across the altitude range and that the model wavelength is slightly shorter than that observed in the radiosonde profiles. Overall, the model provides a reasonable description of the observed GW energy density in the lower stratosphere, though it does not capture all the variability and underestimates the observed peak values.

South Georgia also generates a low-level wake to the lee of the island during this case (such wakes are seen in the lee of many islands globally, for example, Hawaii; e.g., Smith and Grubišić 1993). The model simulations contain many of the features detected in the ASCAT observations, and an extended study over the whole duration of the winter radiosonde campaign period shows this is true in general. There are clear wake signatures downstream of South Georgia during periods of both westerly and northerly flow.

Previous studies (Vosper 2015; Vosper et al. 2016) have indicated the importance of high resolution in modeling orographic GW impacts near South Georgia and have suggested a resolution of 1.5 km (for GW momentum flux) and 3–6 km (for low-level drag) may be required. However, there was an outstanding need to validate such results against detailed local measurements obtained in field campaigns, such as SG-WEX. This has been done here, and we show a high level of agreement between the model and observations. Furthermore, the results indicate that 1.5 km may be the maximum resolution required to simulate GW momentum flux over South Georgia, since our results were largely unchanged when the UM resolution was increased to 750 m.

We can thus have a high degree of confidence in using high-resolution simulations as a “truth” to develop parameterization schemes. This will be important in addressing the ongoing small-island problem in global weather forecast and climate models, which have a coarser resolution (typically several tens of kilometers), and also in properly simulating low-level wakes in the lee of not only South Georgia but also other islands like New Zealand and Hawaii, which can extend several hundreds of kilometers downstream. Parameterizations can be tuned to broadly represent the momentum flux and low-level drag but tend to show less intermittency than the resolved, high-resolution model fields. Further process studies, including further detailed analysis of SG-WEX radiosonde data, shall be carried out to better understand this problem and in particular how the findings from this case study can be generalized.

As part of SG-WEX, a meteor radar has been installed at South Georgia, and, in combination with

the satellite and radiosonde data, this will enable us to observe GWs in the troposphere, stratosphere, and mesosphere over South Georgia. The data gathered as part of SG-WEX provide an exciting opportunity to advance the representation of gravity waves generated by small mountainous islands in models like the UM. Such improvements will allow us to represent significant effects from resolving the small-island problem that will improve climate forecasting

ACKNOWLEDGMENTS. We thank Joan Alexander for helpful comments on draft versions of this paper, and Steve Colwell, the station leader, and staff of King Edward Point Research Station for assistance in planning and carrying out the radiosonde campaign. We would also like to thank the government of South Georgia and the South Sandwich Islands for their cooperation.

The SG-WEX project was supported by the Natural Environment Research Council (NERC) under Grants NE/K015117/1, NE/K012584/1, and NE/K012614/1. We also acknowledge use of the MONSooN system, a collaborative facility supplied under the Joint Weather and Climate Research Programme, a strategic partnership between the Met Office and NERC.

REFERENCES

Alexander, M. J., and C. Barnett, 2007: Using satellite observations to constrain gravity wave parameterizations for global models. *J. Atmos. Sci.*, **64**, 1652–1665, <https://doi.org/10.1175/JAS3897.1>.

—, S. D. Eckermann, D. Broutman, and J. Ma, 2009: Momentum flux estimates for South Georgia Island mountain waves in the stratosphere observed via satellite. *Geophys. Res. Lett.*, **36**, L12816, <https://doi.org/10.1029/2009GL038587>.

—, and Coauthors, 2010: Recent developments in gravity-wave effects in climate models and the global distribution of gravity-wave momentum flux from observations and models. *Quart. J. Roy. Meteor. Soc.*, **136**, 1103–1124, <https://doi.org/10.1002/qj.637>.

Bannister, D., and J. King, 2015: Foehn winds on South Georgia and their impact on regional climate. *Weather*, **70**, 324–329, <https://doi.org/10.1002/wea.2548>.

Buhler, O., 2003: Equatorward propagation of inertia-gravity waves due to steady and intermittent wave sources. *J. Atmos. Sci.*, **60**, 1410–1419, [https://doi.org/10.1175/1520-0469\(2003\)060<1410:EPOIWD>2.0.CO;2](https://doi.org/10.1175/1520-0469(2003)060<1410:EPOIWD>2.0.CO;2).

Dee, D. P., and Coauthors, 2011: The ERA-Interim reanalysis: Configuration and performance of the data assimilation system. *Quart. J. Roy. Meteor. Soc.*, **137**, 553–597, <https://doi.org/10.1002/qj.828>.

Doyle, J. D., and M. A. Shapiro, 1999: Flow response to large-scale topography: The Greenland tip jet. *Tellus*, **51A**, 728–748, <https://doi.org/10.3402/tellusa.v51i5.14471>.

Eckermann, S. D., and Coauthors, 2016: Dynamics of orographic gravity waves observed in the mesosphere over the Auckland Islands during the Deep Propagating Gravity Wave Experiment (DEEPWAVE). *J. Atmos. Sci.*, **73**, 3855–3876, <https://doi.org/10.1175/JAS-D-16-0059.1>.

Ern, M., P. Preusse, M. J. Alexander, and C. D. Warner, 2004: Absolute values of gravity wave momentum flux derived from satellite data. *J. Geophys. Res.*, **109**, D20103, <https://doi.org/10.1029/2004JD004752>.

—, —, J. C. Gille, C. L. Hepplewhite, M. G. Mlynczak, J. M. Russell III, and M. Riese, 2011: Implications for atmospheric dynamics derived from global observations of gravity wave momentum flux in stratosphere and mesosphere. *J. Geophys. Res.*, **116**, D19107, <https://doi.org/10.1029/2011JD015821>.

Fritts, D. C., and M. J. Alexander, 2003: Gravity wave dynamics and effects in the middle atmosphere. *Rev. Geophys.*, **41**, 1003, <https://doi.org/10.1029/2001RG000106>.

—, and Coauthors, 2016: The Deep Propagating Gravity Wave Experiment (DEEPWAVE): An airborne and ground-based exploration of gravity wave propagation and effects from their sources throughout the lower and middle atmosphere. *Bull. Amer. Meteor. Soc.*, **97**, 425–453, <https://doi.org/10.1175/BAMS-D-14-00269.1>.

Geller, M. A., and J. Gong, 2010: Gravity wave kinetic, potential, and vertical fluctuation energies as indicators of different frequency gravity waves. *J. Geophys. Res.*, **115**, D11111, <https://doi.org/10.1029/2009JD012266>.

Grubišić, V., R. B. Smith, and C. Schär, 1995: The effect of bottom friction on shallow-water flow past an isolated obstacle. *J. Atmos. Sci.*, **52**, 1985–2005, [https://doi.org/10.1175/1520-0469\(1995\)052<1985:TEOBFO>2.0.CO;2](https://doi.org/10.1175/1520-0469(1995)052<1985:TEOBFO>2.0.CO;2).

—, J. Sachspurger, and R. M. A. Caldeira, 2015: Atmospheric wake of Madeira: First aerial observations and numerical simulations. *J. Atmos. Sci.*, **72**, 4755–4776, <https://doi.org/10.1175/JAS-D-14-0251.1>.

Hindley, N. P., N. D. Smith, C. J. Wright, D. A. S. Rees, and N. J. Mitchell, 2016: A two-dimensional Stockwell transform for gravity wave analysis of AIRS measurements. *Atmos. Meas. Tech.*, **9**, 2545–2565, <https://doi.org/10.5194/amt-9-2545-2016>.

Hoffmann, L., and M. J. Alexander, 2009: Retrieval of stratospheric temperatures from Atmospheric Infrared Sounder radiance measurements for gravity

- wave studies. *J. Geophys. Res.*, **114**, D07105, <https://doi.org/10.1029/2008JD011241>.
- , A. W. Grimsdell, and M. J. Alexander, 2016: Stratospheric gravity waves at Southern Hemisphere orographic hotspots: 2003–2014 AIRS/Aqua observations. *Atmos. Chem. Phys.*, **16**, 9381–9397, <https://doi.org/10.5194/acp-16-9381-2016>.
- Hosking, J., D. Bannister, A. Orr, J. King, E. Young, and T. Phillips, 2015: Orographic disturbances of surface winds over the shelf waters adjacent to South Georgia. *Atmos. Sci. Lett.*, **16**, 50–55, <https://doi.org/10.1002/asl2.519>.
- Jiang, Q., A. Reinecke, and J. D. Doyle, 2014: Orographic wave drag over the Southern Ocean: A linear theory perspective. *J. Atmos. Sci.*, **71**, 4235–4252, <https://doi.org/10.1175/JAS-D-14-0035.1>.
- Kruse, C. G., and R. B. Smith, 2015: Gravity wave diagnostics and characteristics in mesoscale fields. *J. Atmos. Sci.*, **72**, 4372–4392, <https://doi.org/10.1175/JAS-D-15-0079.1>.
- Lane, T. P., M. J. Reeder, B. R. Morton, and T. L. Clark, 2000: Observations and numerical modelling of mountain waves over the Southern Alps of New Zealand. *Quart. J. Roy. Meteor. Soc.*, **126**, 2765–2788, <https://doi.org/10.1002/qj.49712656909>.
- L'Ecuyer, T. S., and J. H. Jiang, 2010: Touring the atmosphere aboard the A-Train. *Phys. Today*, **63**, 36–41, <https://doi.org/10.1063/1.3463626>.
- Lott, F., and M. J. Miller, 1997: A new subgrid-scale orographic drag parametrization: Its formulation and testing. *Quart. J. Roy. Meteor. Soc.*, **123**, 101–127, <https://doi.org/10.1002/qj.49712353704>.
- Lübken, F.-J., and U. von Zahn, 1991: Thermal structure of the mesopause region at polar latitudes. *J. Geophys. Res.*, **96**, 20 841–20 857, <https://doi.org/10.1029/91JD02018>.
- McFarlane, N. A., 1987: The effect of orographically excited gravity wave drag on the general circulation of the lower stratosphere and troposphere. *J. Atmos. Sci.*, **44**, 1775–1800, [https://doi.org/10.1175/1520-0469\(1987\)044<1775:TEOOEG>2.0.CO;2](https://doi.org/10.1175/1520-0469(1987)044<1775:TEOOEG>2.0.CO;2).
- McLandsress, C., T. G. Shepherd, S. Polavarapu, and S. R. Beagley, 2012: Is missing orographic gravity wave drag near 60°S the cause of the stratospheric zonal wind biases in chemistry–climate models? *J. Atmos. Sci.*, **69**, 802–818, <https://doi.org/10.1175/JAS-D-11-0159.1>.
- Moore, G. W. K., and I. A. Renfrew, 2005: Tip jets and barrier winds: A QuikSCAT climatology of high wind speed events around Greenland. *J. Climate*, **18**, 3713–3725, <https://doi.org/10.1175/JCLI3455.1>.
- Palmer, T. N., G. J. Shutts, and R. Swinbank, 1986: Alleviation of a systematic westerly bias in general circulation and numerical weather prediction models through an orographic gravity-wave drag parametrization. *Quart. J. Roy. Meteor. Soc.*, **112**, 1001–1039, <https://doi.org/10.1002/qj.49711247406>.
- Pautet, P.-D., and Coauthors, 2016: Large-amplitude mesospheric response to an orographic wave generated over the Southern Ocean Auckland Islands (50.7°S) during the DEEPWAVE project. *J. Geophys. Res. Atmos.*, **121**, 1431–1441, <https://doi.org/10.1002/2015JD024336>.
- Plougonven, R., A. Hertzog, and L. Guez, 2013: Gravity waves over Antarctica and the Southern Ocean: Consistent momentum fluxes in mesoscale simulations and stratospheric balloon observations. *Quart. J. Roy. Meteor. Soc.*, **139**, 101–118, <https://doi.org/10.1002/qj.1965>.
- Schär, C., and R. B. Smith, 1993: Shallow-water flow past isolated topography. Part I: Vorticity production and wake formation. *J. Atmos. Sci.*, **50**, 1373–1400, [https://doi.org/10.1175/1520-0469\(1993\)050<1373:SWFPIT>2.0.CO;2](https://doi.org/10.1175/1520-0469(1993)050<1373:SWFPIT>2.0.CO;2).
- , and D. Durran, 1997: Vortex formation and vortex shedding in continuously stratified flows past isolated topography. *J. Atmos. Sci.*, **54**, 534–554, [https://doi.org/10.1175/1520-0469\(1997\)054<0534:VFAVS I>2.0.CO;2](https://doi.org/10.1175/1520-0469(1997)054<0534:VFAVS I>2.0.CO;2).
- Scinocca, J. F., and N. A. McFarlane, 2000: The parametrization of drag induced by stratified flow over anisotropic orography. *Quart. J. Roy. Meteor. Soc.*, **126**, 2353–2393, <https://doi.org/10.1002/qj.49712656802>.
- Shutts, G. J., and S. B. Vosper, 2011: Stratospheric gravity waves revealed in NWP model forecasts. *Quart. J. Roy. Meteor. Soc.*, **137**, 303–317, <https://doi.org/10.1002/qj.763>.
- Smith, R. B., and V. Grubišić, 1993: Aerial observations of Hawaii's wake. *J. Atmos. Sci.*, **50**, 3728–3750, [https://doi.org/10.1175/1520-0469\(1993\)050<3728:AOOH W>2.0.CO;2](https://doi.org/10.1175/1520-0469(1993)050<3728:AOOH W>2.0.CO;2).
- Vincent, R., S. Allen, and S. Eckermann, 1997: Gravity-wave parameters in the lower stratosphere. *Gravity Wave Processes and Their Parameterization in Global Climate Models*, K. Hamilton, Ed., Springer-Verlag, 7–25.
- Vosper, S. B., 2015: Mountain waves and wakes generated by South Georgia: Implications for drag parametrization. *Quart. J. Roy. Meteor. Soc.*, **141**, 2813–2827, <https://doi.org/10.1002/qj.2566>.
- , A. R. Brown, and S. Webster, 2016: Orographic drag on islands in the NWP mountain grey zone. *Quart. J. Roy. Meteor. Soc.*, **142**, 3128–3137, <https://doi.org/10.1002/qj.2894>.
- Wang, L., M. A. Geller, and M. J. Alexander, 2005: Spatial and temporal variations of gravity wave parameters. Part I: Intrinsic frequency, wavelength,

- and vertical propagation direction. *J. Atmos. Sci.*, **62**, 125–142, <https://doi.org/10.1175/JAS-3364.1>.
- Webster, S., A. R. Brown, D. R. Cameron, and C. P. Jones, 2003: Improvements to the representation of orography in the Met Office Unified Model. *Quart. J. Roy. Meteor. Soc.*, **129**, 1989–2010, <https://doi.org/10.1256/qj.02.133>.
- Wells, H., S. B. Vosper, S. Webster, A. N. Ross, and A. R. Brown, 2008a: The impact of mountain wakes on the drag exerted on downstream mountains. *Quart. J. Roy. Meteor. Soc.*, **134**, 677–687, <https://doi.org/10.1002/qj.242>.
- , —, A. N. Ross, A. R. Brown, and S. Webster, 2008b: Wind direction effects on orographic drag. *Quart. J. Roy. Meteor. Soc.*, **134**, 689–701, <https://doi.org/10.1002/qj.247>.
- Wood, N. A., and Coauthors, 2014: An inherently mass-conserving semi-implicit semi-Lagrangian discretization of the deep-atmosphere global non-hydrostatic equations. *Quart. J. Roy. Meteor. Soc.*, **140**, 1505–1520, <https://doi.org/10.1002/qj.2235>.
- Wright, C. J., N. P. Hindley, and N. J. Mitchell, 2016: Combining AIRS and MLS observations for three-dimensional gravity wave measurement. *Geophys. Res. Lett.*, **43**, 884–893, <https://doi.org/10.1002/2015GL067233>.
- , —, L. Hoffmann, M. J. Alexander, and N. J. Mitchell, 2017: Exploring gravity wave characteristics in 3-D using a novel S-transform technique: AIRS/Aqua measurements over the Southern Andes and Drake Passage. *Atmos. Chem. Phys.*, **17**, 8553–8575, <https://doi.org/10.5194/acp-17-8553-2017>.
- Young, G. S., and J. Zawislak, 2006: An observational study of vortex spacing in island wake vortex sheets. *Mon. Wea. Rev.*, **134**, 2285–2294, <https://doi.org/10.1175/MWR3186.1>.
- Zink, F., and R. A. Vincent, 2001: Wavelet analysis of stratospheric gravity wave packets over Macquarie Island: 1. Wave parameters. *J. Geophys. Res.*, **106**, 10 275–10 288, <https://doi.org/10.1029/2000JD900847>.

NEW FROM AMS BOOKS!

The Thinking Person's Guide to Climate Change

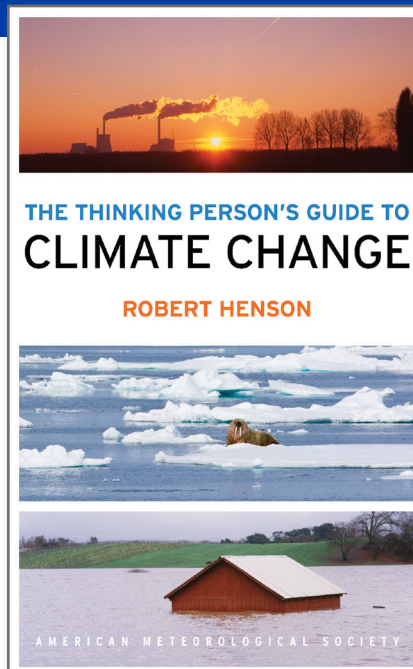
Robert Henson

Expanded and updated from Henson's *Rough Guide to Climate Change*, 3rd edition (no longer in print), combining years of data with recent research, including conclusions from the Fifth Assessment Report of the Intergovernmental Panel on Climate Change, the Guide breaks down the issues into straightforward categories:

- Symptoms, including melting ice and extreme weather
- Science, laying out what we know and how we know it
- Debates, tackling the controversy and politics
- Solutions and Actions for creating the best possible future

© 2014, 516 pages, paperback
ISBN: 978-1-878220-73-7

List price: \$30 AMS Member price: \$20



AMS BOOKS

RESEARCH APPLICATIONS HISTORY

➤ bookstore.ametsoc.org



Anniversary Campaign

Imagine the potential
Engage the world
Empower the future

*Help us
empower the future
of the atmospheric, oceanic,
and hydrologic sciences*

In 2019, AMS will celebrate our 100th Anniversary. To mark this incredible milestone, we're inviting our members and others across the weather, water, and climate community to join us in supporting the future success of scientists, professionals, students, educators, broadcasters and others committed to using science to make the world a better place.

The AMS 100th Anniversary Campaign is raising funds in critical areas to ensure our fields of science are well-positioned to help meet the challenges of a changing world. There are a number of ways to contribute either now or as future giving.

Please consider giving to any of our campaign funds:

- **Rapid Adaptation**
- **Breakthrough Science**
- **Engaging the Public**
- **Bridging Disciplines**
- **Globalization**



AMS
American Meteorological Society

ametsoc.org/give

AMS BOOKS

RESEARCH APPLICATIONS HISTORY

AMS MEMBERS GET FREE

CLIMATE

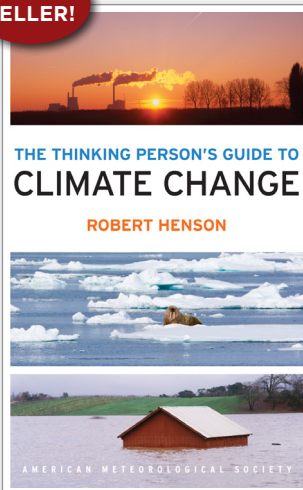
The Thinking Person's Guide to Climate Change

ROBERT HENSON

This fully updated and expanded revision of *The Rough Guide to Climate Change* combines years of data with recent research. It is the most comprehensive overview of climate science, acknowledging controversies but standing strong in its stance that the climate is changing—and something needs to be done.

© 2014, PAPERBACK, 520 PAGES,
ISBN: 978-1-935704-73-7
LIST \$30 MEMBER \$20

BEST
SELLER!

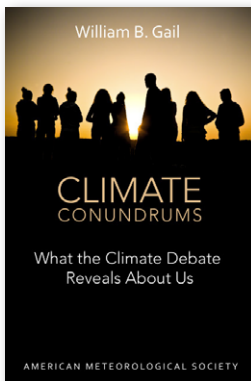


Climate Conundrums: What the Climate Debate Reveals about Us

WILLIAM B. GAIL

This is a journey through how we think, individually and collectively, about humanity's relationship with nature, and more. Can we make nature better? Could science and religion reconcile? Gail's insights on such issues help us better understand who we are and find a way forward.

© 2014, PAPERBACK, 240 PAGES,
ISBN: 978-1-935704-74-4 LIST \$30 MEMBER \$20

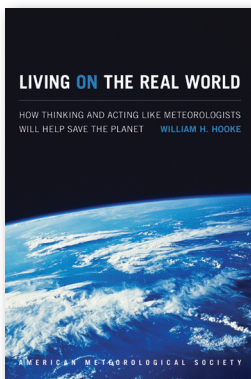


Living on the Real World: How Thinking and Acting Like Meteorologists Will Help Save the Planet

WILLIAM H. HOOKE

Meteorologists focus on small bits of information while using frequent collaboration to make decisions. With climate change a reality, William H. Hooke suggests we look to the way meteorologists operate as a model for how we can solve the 21st century's most urgent environmental problems.

© 2014, PAPERBACK, 272 PAGES, ISBN 978-1-935704-56-0 LIST \$30 MEMBER \$22



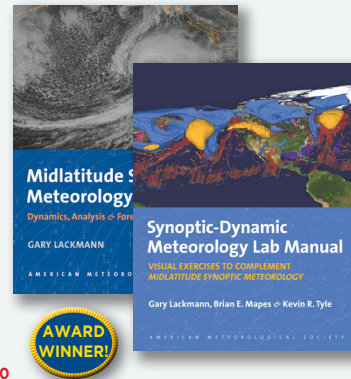
Synoptic-Dynamic Meteorology Lab Manual: Visual Exercises to Complement Midlatitude Synoptic Meteorology

GARY LACKMANN,
BRIAN E. MAPES, AND
KEVIN R. TYLE

These labs link theoretical concepts with ground-breaking visualization to elucidate concepts taught in the award-winning companion textbook by Gary Lackmann, *Midlatitude Synoptic Meteorology*.

© 2017, PAPERBACK, 126 PAGES,
ISBN 978-1-878220-26-4

LIST \$80 MEMBER \$60 STUDENT \$50



GUIDES

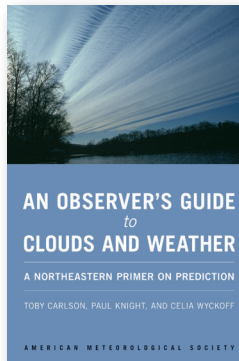
An Observer's Guide to Clouds and Weather:

A Northeastern Primer on Prediction

TOBY CARLSON, PAUL KNIGHT,
AND CELIA WYCKOFF

With help from Penn State experts, start at the beginning and go deep. This primer, intended for both serious enthusiasts and new meteorology students, will leave you with both refined observation skills and an understanding of the complex science behind the weather: the ingredients for making reliable predictions of your own. It connects fundamental meteorological concepts with the processes that shape weather patterns, and will make an expert of any dedicated reader.

© 2014, PAPERBACK, 210 PAGES,
ISBN: 978-1-935704-58-4 LIST \$30 MEMBER \$20



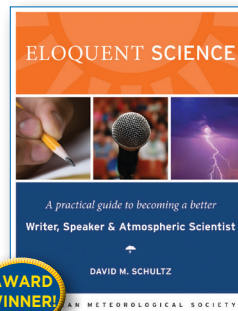
Eloquent Science: A Practical Guide to Becoming a Better Writer, Speaker, and Atmospheric Scientist

DAVID M. SCHULTZ

The ultimate communications manual for undergraduate and graduate students as well as researchers in the atmospheric sciences and their intersecting disciplines.

© 2009, PAPERBACK, 440 PAGES,
ISBN 978-1-878220-91-2

LIST \$45 MEMBER \$30



To order: bookstore.ametsoc.org, 617-226-3998, or use the order form in this magazine

NEW

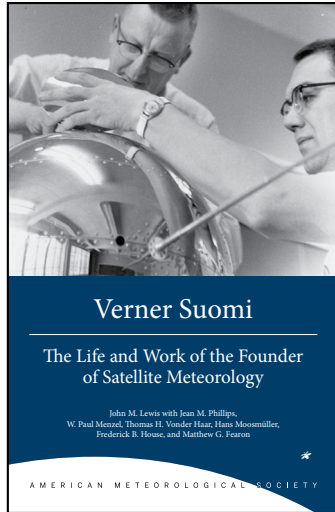
**Verner Suomi:
The Life and Work
of the Founder of
Satellite Meteorology**

JOHN M. LEWIS WITH
JEAN M. PHILLIPS, W. PAUL
MENZEL, THOMAS H. VONDER
HAAR, HANS MOOSMÜLLER,
FREDERICK B. HOUSE,
AND MATTHEW G. FEARON

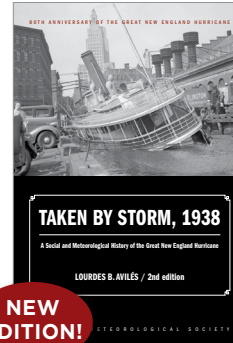
Born in a Minnesotan mining town, Suomi would spend his best years next door in Wisconsin, but not before seeing the whole world—from space, that is. This is the story of the scientist, inventor, and teacher who founded satellite meteorology, written by members of the communities that grew up around his groundbreaking work.

LIST \$30 MEMBER \$20

© 2016, PAPERBACK, 240 PAGES, ISBN: 978-1-944970-22-2



HISTORY



NEW EDITION!

**Taken by Storm, 1938:
A Social and Meteorological History of the Great New England Hurricane, 2nd Ed.**

LOURDES B. AVILÉS

80TH ANNIVERSARY OF STORM

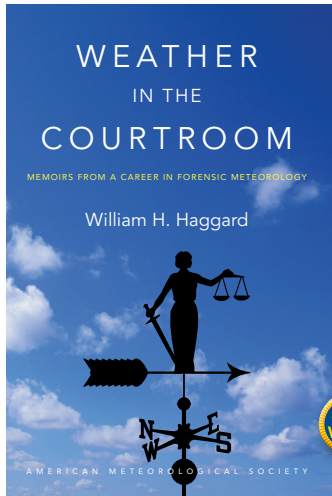
The science behind the 1938 Hurricane, which hit New England unannounced, is presented here for the first time along with new data that

sheds light on the motivations of the Weather Bureau forecasters. This compelling history successfully weaves science, historical accounts, and social analyses to create a comprehensive picture of the most powerful and devastating hurricane to hit New England to date.

© 2018, PAPERBACK, 288 PAGES, ISBN: 978-1-944970-24-6

LIST \$30 MEMBER \$20

Weather in the Courtroom: Memoirs from a Career in Forensic Meteorology



WILLIAM H. HAGGARD

From a pioneering forensic meteorologist, the inside scoop on legendary litigations, including the disappearance of an Alaskan congressman's airplane in 1972, the collapse of Tampa Bay's Skyway Bridge in 1980, and the crash of Delta Flight 191 in Dallas/Fort Worth in 1985.

LIST \$30 MEMBER \$20

© 2016, PAPERBACK, 240 PAGES, ISBN: 978-1-940033-95-2

AWARD WINNER!

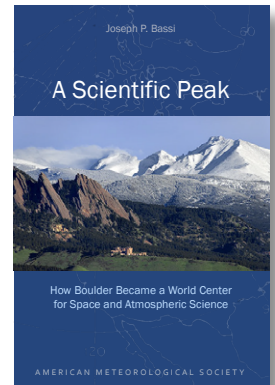
**A Scientific Peak:
How Boulder Became a World Center for Space and Atmospheric Science**

JOSEPH P. BASSI

How did big science come to Boulder, Colorado? Joe Bassi introduces us to the characters, including Harvard sun-Earth researcher Walter Orr Roberts, and the unexpected brew of politics, passion, and sheer luck that during the Cold War era transformed this "Scientific Siberia" to home of NCAR and NOAA.

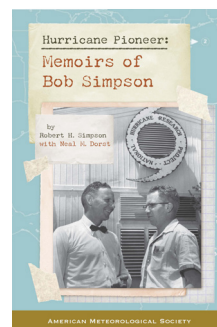
© 2015, PAPERBACK, 264 PAGES, ISBN: 978-1-935704-85-0

LIST PRICE: \$35.00 MEMBER PRICE: \$25.00



**Hurricane Pioneer:
Memoirs of Bob Simpson**

ROBERT H. SIMPSON AND NEAL DORST



In 1951, Bob Simpson rode a plane into a hurricane—just one of the many pioneering exploits you'll find in these memoirs. Bob and his wife Joanne are meteorological icons: Bob was the first director of the National Hurricane Research Project and a director of the National Hurricane Center. He helped to create the Saffir-Simpson Hurricane Scale; the

public knows well his Categories 1-5. Proceeds from this book help support the AMS's K. Vic Ooyama Scholarship Fund.

© 2015, PAPERBACK, 156 PAGES

ISBN: 978-1-935704-75-1

LIST \$25

MEMBER \$20



**Booksellers, groups,
or for examination copies:**

The University of Chicago Press:
1-800-621-2736 (US & Canada)
773-702-7000 (all others)
custserv@press.uchicago.edu



MORE THAN 21,000 TEACHERS DIRECTLY TAUGHT

MILLIONS OF STUDENTS BENEFIT

OVER 150,000 TEACHERS PEER TRAINED



K-12 Teachers,
 Enhance your knowledge of Earth system science and earn tuition free graduate credits through AMS Education's teacher professional development program. Learn about fundamental weather, ocean, or climate topics through a distance-learning course emphasizing the study of Earth system science as it happens and discover ways to instill the excitement of real-world information across your science curriculum.

ENROLL IN A FREE DATASTREME COURSE TODAY. Register by **JULY 28TH** to be connected with a Local Implementation team before the courses begin on August 28th.

Learn more: ametsoc.org/datastreme

Questions: amsedu@ametsoc.org